Electronic Energy Changes Associated with Guanine Quadruplex Formation: An Investigation at the Atomic Level

Alexis Taylor,[†] Justine Taylor,[‡] Graeme W. Watson,[‡] and Russell J. Boyd*,[†]

Department of Chemistry, Dalhousie University, Halifax, NS, Canada B3H 4J3, School of Chemistry, Trinity College, University of Dublin, Dublin 2, Ireland

Received: December 20, 2009; Revised Manuscript Received: June 13, 2010

Guanine quadruplexes have received a lot of attention due to their possible role as therapeutic agents. Specifically, it is the ability of these quadruplex structures to inhibit telomerase, an enzyme found to be highly active in a large percentage of tumor cells and thought to confer immortality upon these cells. However, although a great deal of research has focused on enhancing the formation of these structures and their anticancer activity, many questions remain about the quadruplex structures themselves. The current study probes the nature of these quadruplex structures at the atomic level. Individual atomic energies have been computed for the quadruplex structure and compared to the atomic energies of the unfolded telomere to determine the energetic consequences of quadruplex formation. The results suggest several interesting trends, most notably that the guanine quartets exhibit an alternating pattern of stabilization and destabilization and these regions actually overlap in the intact quadruplex. In addition, the TTA loop segments are largely stabilized, whereas the atoms in the sugar−phosphate backbone exhibit mostly minor changes going from the unfolded to folded state. Inclusion of additional sodium cations in the central core of the quadruplex has a minimal effect on the atomic energies except for the atoms that are closest to the cations, which are largely stabilized in the presence of these ions.

1. Introduction

Human chromosomes are capped at their ends with guanine-rich tracts of DNA known as telomeres.[1] These segments protect the chromosomes from losing important genetic information during successive rounds of replication, a consequence of the end-replication problem.[2] Although a large portion of the telomere is bound to a complementary cytosine-rich tract of DNA, the 3′ terminus exists as a single-stranded overhang.[3,4] Due to the propensity of guanine to form quartets,[5] as shown in Figure 1, these G-rich tracts of DNA can form unique guanine quadruplex (G-quadruplex) structures by stacking several quartets and may be stabilized by various metal cations.[6] The variety of structures observed is large due to the polymorphic nature of these systems, differing in the strand orientation (parallel versus antiparallel), the glycosidic conformation (syn/anti), and the loop connections (diagonal, edge-wise, double-chain reversals, etc.).[7,8] Although direct evidence for the formation of G-quadruplexes in vivo is still lacking, the indirect evidence continues to mount. For instance, proteins that can bind to G-quadruplexes[9,10] have been observed as well as helicases[11] and nucleases[12] that act specifically on these structures. However, the most compelling evidence to date has been the generation[13] and subsequent reaction in vivo[14] of a G-quadruplex specific antibody.

During normal cell growth, the length of a telomere can be used as an indication of the age and viability of a cell;[15−17] once a certain crisis length is reached, senescence and even cell death may be triggered. However, a specialized RNA-dependent enzyme called telomerase is capable of maintaining and extending telomeres,[18−20] a mechanism that is required for the uncontrolled cell growth observed in cancerous cells. In fact, nearly 85% of all tumor cells exhibit high levels of telomerase, whereas this enzyme is generally inactive in somatic cells.[21] Furthermore, it has been observed that quadruplex structures inhibit telomerase.[22−27] As such, telomerase, and telomeres themselves, have become viable targets for selective therapeutic strategies.[28−31] Several studies have found that ligands known to bind to G-quadruplex structures have already shown anticancer activity.[32−36]

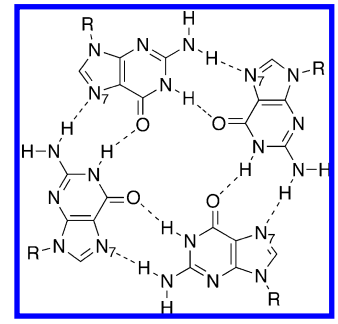

Figure 1. Guanine quartet formed from Watson−Crick hydrogen bonds as well as Hoogsteen hydrogen bonds through N7.

G-quadruplex structures are suspected to form not only in telomeric sequences but also in many other guanine-rich regions of DNA. Analysis of the entire human genome suggests there may be upward of 376 000 sequences capable of forming quadruplexes.[37,38] Furthermore, 40% of all genes contain potential G-quadruplex forming sequences in their promoters.[39] Should such a structure form in this region, the gene could no longer be expressed, and thus, G-quadruplexes may ultimately play a role in gene regulation at the level of transcription. Also of interest is the fact that these sequences are observed more frequently in proto-oncogenes and less frequently in tumor

* Corresponding author. E-mail: russell.boyd@dal.ca.
[†] Dalhousie University.
[‡] University of Dublin.

10.1021/jp912013k
Published on Web 07/08/2010

suppressor genes,[40] once again implicating the G-quadruplex as a possible therapeutic target. The ubiquitous nature of G-rich segments in the human genome demands attention and requires a thorough understanding of these species.

The current investigation probes the energetic consequences of quadruplex formation at the atomic level. The theory of atoms in molecules (AIM) has been used to determine the atomic properties of the unfolded, single-stranded telomere and the intramolecularly folded guanine quadruplex observed via NMR in sodium solution.[41] Although several different quadruplex structures have been obtained experimentally, the current study focuses specifically on an antiparallel, basket-type structure. Comparison of the atomic energies between these two systems will be used to illustrate which regions of the telomere are stabilized or destabilized upon quadruplex formation. Ultimately, this information may lead to suggestions for potential therapeutic targets. For instance, should a particular region of the telomere be destabilized upon folding, a small molecule could be developed to bind to this region and stabilize it in an effort to enhance quadruplex formation.

2. Computational Details

The initial structure of the intramolecular quadruplex, $AG_3(T_2AG_3)_3$, was obtained from Protein Data Bank (PDB) entry 143D, an NMR structure in sodium solution as determined by Wang and Patel.[41] Of the six structures deposited for entry 143D, the first structure was selected because it was the most compact structure, with the majority of the loop nucleobases oriented toward the central guanine quartet core. Subsequently, a constrained energy minimization was performed on the hydrogen and sodium atoms using AM1[42,43] while all heavy atoms other than sodium remained fixed. It was assumed that further optimization of the heavy atoms using AM1 would provide no additional benefit compared to the coordinates determined from the experimental data. The resultant structures were then subject to single-point energy calculations at the B971/6-31+G(d,p) level of theory using the Gaussian 03 suite of programs.[44] The B971 functional[45] was selected on the basis of its performance in a previous study on hydrogen bonding.[46] Due to the large size of the system, the structure was decomposed into smaller fragments so that the single-point calculations could be completed using the available resources. The fragments were chosen such that for a particular region under investigation, the adjacent nucleobases on either side were included. For example, when the central guanine quartet was examined, both of the surrounding quartets as well as the sugar−phosphate backbone were included in the structure. All fragments were capped with hydrogen atoms. Further description of the fragments can be found in the Supporting Information. The theory of atoms in molecules, as implemented in AIMPAC,[47] was used to analyze the electron densities obtained.

The theory of atoms in molecules is based on the topological analysis of the electron density using the gradient.[48,49] This type of analysis allows for the partitioning of a system into fragments, which ultimately define the individual atoms. This partitioning is achieved by the determination of the interatomic surfaces (IAS), which must satisfy a zero-flux condition,

$$\nabla\rho(\mathbf{r})\cdot\mathbf{n}(\mathbf{r}) = 0 \qquad (1)$$

where $\nabla\rho(\mathbf{r})$ is the gradient of the electron density and $\mathbf{n}(\mathbf{r})$ is a unit vector normal to the surface. The region enclosed by the interatomic surface and the attractor (i.e., the nucleus) found within this boundary define the atomic basin. This mathematically rigorous partitioning of the system into atomic basins allows for the determination of the atomic contributions to a given molecular property simply by integrating the property of interest over the atomic basin. Specifically, in this study, AIM was used extensively to calculate the individual atomic energies in the single-stranded telomere and the quadruplexes. For a more complete introduction to the theory of atoms in molecules, we refer the reader to Chapter 1 in ref 49.

TABLE 1: Equilibration Protocol

time	ensemble	temperature (K)	restrained atoms	force constant (kcal mol^{-1} Å^{-2})
20 ps	NPT	100	all but water	500
5000 steps	minimization		all but water	500
5000 steps	minimization		none	
20 ps	NPT	100	DNA	100
20 ps	NPT	300	DNA	100
10 ps	NPT	300	DNA	50
10 ps	NPT	300	DNA	25
10 ps	NPT	300	DNA	10
10 ps	NPT	300	DNA	5
10 ps	NPT	300	DNA	1
14 ps	NPT	300	none	

To compare the atomic energies of the unfolded, single-stranded telomere and the quadruplex structure, a single-stranded reference system is required. Unfortunately, structural data of a single-stranded telomere in solution was not available and thus had to be generated during this study. To this end, the preferred structure of a single-stranded segment of telomeric DNA in solution was obtained from molecular dynamics simulations. The reference system used in this study consisted of a tract of telomeric DNA capped with two nucleobases at each end, resulting in an overall sequence of 5′-TAGGGTTAGG-3′. This was extracted from the DNA component of the first deposited structure in PDB entry 1VFC.[50] The structure was protonated, solvated (10 657 waters), and neutralized with Na^+ counterions using the AMBER9[51,52] Leap module. DNA was described by the PARMBSC0 force field;[53] water, by TIP3P;[54] and the sodium ions, by the standard AMBER-99 force field.[55] The system was equilibrated using a multistage protocol, shown in Table 1, based on that described by Shields et al.[56]

Three independent 30 ns simulations were run starting from the 10, 12, and 14 ps time points of the final equilibration phase. All simulations were performed using the AMBER9 PMEMD module with periodic boundaries, and the particle mesh Ewald (PME) method[57,58] was used to evaluate the electrostatics with grid points set no more than 1 Å apart. The cutoff radius for nonbonded interactions was 12 Å with nonbonded list updates every 25 steps. SHAKE was used with a tolerance of 0.000 01 to constrain all bonds involving hydrogen, allowing for an integration step of 2 fs. Langevin dynamics with a collision frequency of 1 ps^{-1} was used to maintain a simulation temperature of 300 K. Isotropic position scaling with a relaxation time of 2.0 ps was used to maintain a pressure of 1 atm.

Snapshots were collected every 2 ps over the full 30 ns for each simulation and were least-squares-fitted to the DNA backbone of the starting structure. Structures were clustered using the backbone only with a fixed cluster radius of 4 Å using the MMTSB toolset.[59] Using the most highly populated cluster, the snapshot with the lowest rmsd to the centroid structure was taken as the starting point for the electronic structure calculations. This structure was then subjected to a constrained optimization of the hydrogen atoms using AM1 followed by a single-point energy calculation at the B971/6-31+G(d,p) level of theory.

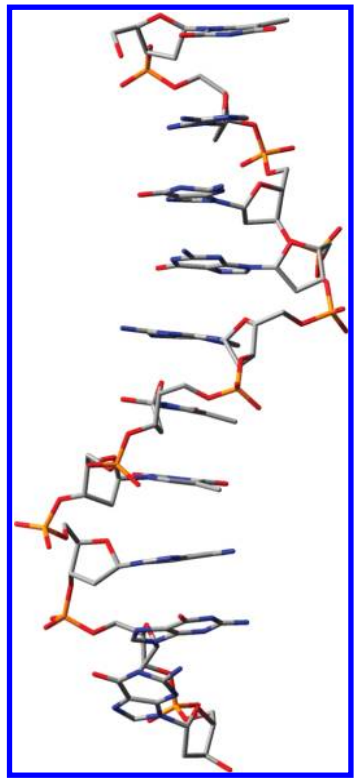

Figure 2. Final structure of the single-stranded telomere sequence, 5′-TAGGGTTAGG-3′. The hydrogen atoms have been omitted for clarity.

3. Results and Discussion

3.1. Structure of the Single-Stranded Telomere Sequence. The final structure of the single-stranded telomere (sequence 5′-TAGGGTTAGG-3′) reveals that it remains relatively linear, as shown in Figure 2. The telomere adopts a helical structure, with adjacent nucleobases essentially parallel and aligned, suggesting that the stacking interactions present in duplex DNA are maintained in the single-stranded segment. The nucleobase at the 3′ end of the telomere is slightly puckered and tilted toward the adjacent nucleobase. This disruption of the parallel stacking is likely due to end effects; however, it is not likely to affect the results of this study, since only the central nucleobases in this segment were used as the reference system. The coordinates of this telomere structure are available in the Supporting Information. The atomic energies of the single-stranded telomere were determined (data not shown) and served as a reference for comparison to the atomic energies in the quadruplex structures.

3.2. Atomic Energy Differences for the Guanine Quadruplex. The intramolecular quadruplex investigated in this study, $G_3(T_2AG_3)_3$, forms a basket-type structure in sodium solution. This quadruplex consists of three stacked guanine quartets connected by one diagonal and two lateral TTA loops, as shown in Figure 3. Using the electron density obtained from the single-point energy calculations, the atomic energy of each atom in the quadruplex was calculated. To determine whether a particular atom is stabilized or destabilized upon quadruplex formation, its energy was compared with the energy of the corresponding atom in the single-stranded telomere. The difference between these two values, ΔE, where $\Delta E = E$(atom in quadruplex) $- E$(atom in ssDNA), is reported in the Supporting Information as the atomic energy differences. A table of how the nucleobases were compared between the quadruplex and single-stranded DNA is also provided in the Supporting Information. If the atom is stabilized upon folding into the quadruplex structure, the energy difference is consequently negative, and conversely, if the atom is destabilized, the energy difference must be positive.

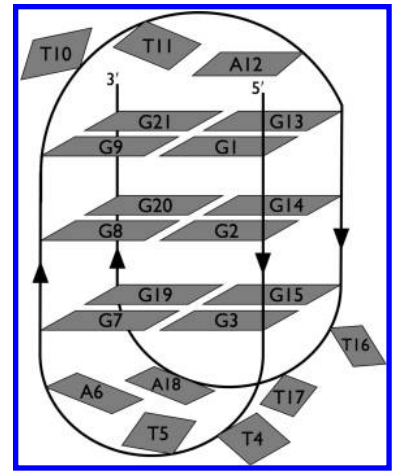

Figure 3. Schematic illustration of the intramolecular, basket-type quadruplex illustrating the numbering scheme used for the nucleobases.

To more easily analyze the plethora of data obtained in this study, a novel means of displaying the atomic energy differences had to be devised. Simply scanning through the tables of data gave little indication of any trends present in the folded quadruplex. To this end, we have chosen to graphically illustrate the energy differences using the coordinates of the quadruplex and spheres that have been both color- and size-coded to represent the sign and magnitude of the energy difference, respectively. Atoms that are stabilized upon quadruplex formation appear as red spheres, and those that are destabilized appear as blue spheres. The magnitude of the energy difference corresponds directly with the size of the sphere: the larger the change in energy, the larger the sphere. Those atoms that are essentially unaffected by the change in structure are represented by small, black spheres. Considering the range of energy differences observed, changes of 20 kJ/mol or less were deemed sufficiently small to be considered unchanged for the purpose of this study. The final result for the intact quadruplex is shown in Figure 4. This novel method of displaying the energy differences has allowed the visualization in three dimensions of how the individual atoms are affected by folding into the quadruplex, and it permits the easy identification of any patterns or trends in the energy changes.

Although it is not immediately apparent from Figure 4, there are several trends in the atomic energy differences that would not have been identified unless the energies were plotted in such a 3D fashion. For instance, the guanine quartets exhibit an alternating pattern of stabilization and destabilization around the ring of the quartet. This can be seen easily once the loop segments and the sugar−phosphate backbone have been stripped away, as shown in Figure 5. Furthermore, not only does each individual quartet exhibit such a pattern (Figure 5c−e), but also the regions actually overlap with one another when the quartets are stacked in the intact quadruplex (Figure 5a and b).

A quick visual inspection of Figure 5c−e suggests that the red spheres are slightly dominant in the top and bottom guanine quartets (Figure 5c and e), and the blue spheres are more prevalent in the middle quartet (Figure 5d). Summing up the individual atomic energy differences over the quartets confirms these suspicions. The top and bottom quartets are stabilized by

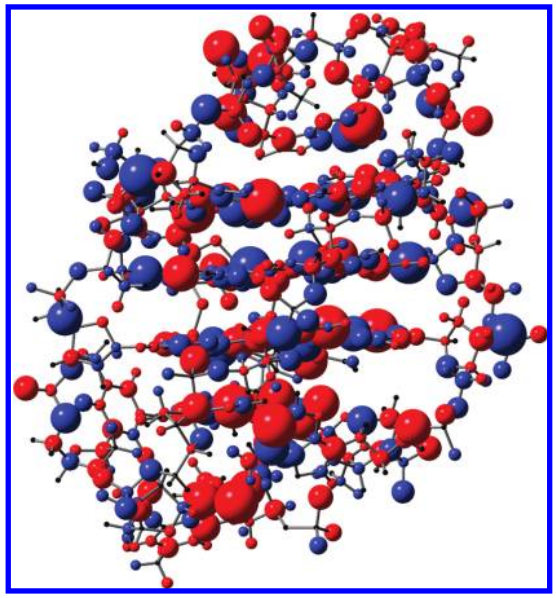

Figure 4. Graphical representation of the atomic energy differences, ΔE, for the intact quadruplex. Atoms that are stabilized appear as red spheres, those that are destabilized are blue, and those that are essentially unchanged appear as black spheres. The magnitude of the energy difference correlates directly with the size of the sphere used.

−230.3 and −294.8 kJ/mol, respectively, and the middle guanine quartet is significantly destabilized by 1828.8 kJ/mol.

Examining the loop regions more closely also presents another unexpected trend. It was initially hypothesized that the loop segments would be destabilized upon quadruplex formation due to the fact that the nucleobases involved would lose the favorable stacking interactions they possess in the single-stranded telomere. However, once the atomic energies were plotted on the intact quadruplex, it became clear that, in fact, the opposite is true. All three TTA loop regions are largely stabilized in the folded quadruplex, indicating that the weak stacking interactions are replaced by stronger, more favorable interactions. Figure 6a−c illustrates that the red spheres dominate the image in the loop regions. Once again, the stabilization in these loop regions can be quantified by summing up the atomic energy differences. Focusing on the atoms in the nucleobases, each TTA loop is stabilized by roughly −2300 kJ/mol.

Finally, looking at the sugar−phosphate backbone, there does not appear to be any obvious trend in the atomic energy differences. It was noted that the O3′ and O5′ oxygens of the guanine nucleotides are often largely destabilized throughout the backbone of the quadruplex. Otherwise, the magnitude of the energy differences are, on average, smaller than those observed for the atoms in the nucleobases. This finding makes sense since the atoms in the backbone have not been disturbed greatly upon quadruplex formation, as compared with the atoms in the nucleobases. Overall, the atoms in the sugar−phosphate backbone have a destabilizing contribution of 1138.5 kJ/mol.

Summing up the individual atomic energy differences observed over the entire quadruplex indicates that this structure is significantly stabilized relative to the single-stranded telomere. Collectively, the atomic energy differences result in a stabilization of −4523.3 kJ/mol.

3.3. Addition of Sodium Cations. Since the experimental structure was obtained in sodium solution, additional quadruplex structures that included sodium cations during the constrained energy minimization were investigated. Although there are various studies in the literature that investigate the preferred binding mode of metal cations to isolated nucleobase quartets,[60−64] little is known about the exact location and number of cations found within G-quadruplex structures.[65,66] On the basis of this information, three additional systems with varying numbers of sodium cations were investigated. Initially, the sodium cations were placed in the plane of the guanine quartets. However, the final optimized structures reveal that the sodium cations prefer a position between the stacked quartets or within the cavity formed by the loop segments and an external quartet, as shown in Figure 7.

Atomic energies were calculated for these systems, and the energy differences between the folded quadruplex and the single-stranded telomere were computed. The detailed atomic energy differences are available in the Supporting Information. To visualize the effect of the additional sodium cations, the energy differences between the systems with sodium cations and the quadruplex without any additional ions were compared and graphically displayed in the same manner as discussed previously. In this case, the difference in energy differences, $\Delta(\Delta E)$, has been plotted, where $\Delta(\Delta E) = \Delta E$(quadruplex with Na^+ ions) − ΔE(quadruplex without ions). Any additional stabilization upon the inclusion of the sodium cations is again indicated using red spheres with the size of the sphere corresponding to the magnitude of the energy change. Conversely, destabilization is indicated using blue spheres, and for those atoms that exhibit minimal changes in energy (e.g., <20 kJ/mol), the spheres appear black.

Upon the inclusion of additional sodium cations, relatively few changes were observed. Most notably, the atoms closest to the sodium ions were stabilized. Except for the carbonyl oxygen atoms on guanine, which exhibited large energy changes, the $\Delta(\Delta E)$ values were quite small in magnitude, and any changes greater than 20 kJ/mol were fairly sparse. As can be seen in Figure 8, as the number of sodium cations increases, the number of significant $\Delta(\Delta E)$ values increases, and their effect is propagated further throughout the quadruplex. For instance, the system with only two additional sodium cations exhibits large $\Delta(\Delta E)$ values only among the guanine nucleobases in the stacked quartets, whereas the systems with three or four cations also exhibit significant changes in the loop nucleobases. In all cases, the atoms in the sugar−phosphate backbone are essentially unaffected by the presence or absence of sodium cations. Although the changes are relatively short-ranged and smaller, collectively, they result in a significant stabilization. Relative to the quadruplex without any sodium cations, the two-, three-, and four-cation systems are stabilized by −2255.7, −2877.7, and −3691.7 kJ/mol, respectively.

4. Conclusion

Although guanine quadruplexes have been investigated extensively for their therapeutic properties, many questions remain about the nature of the quadruplex structures themselves. In an attempt to better understand why these structures might form, the current study investigates the energetic consequences of quadruplex formation on an atom-by-atom basis. This goal was achieved by comparing the atomic energies of the single-stranded telomere to those in the folded quadruplex. The atomic energy differences between these two systems reveal several interesting trends. However, to elucidate these trends, a novel means of displaying the atomic data had to be devised. This was accomplished by representing the energy differences with spheres whose size and color corresponded to the magnitude and sign of the change, respectively. These data were then plotted using the coordinates of the intact quadruplex to visualize the changes in three dimensions. The results indicate that the

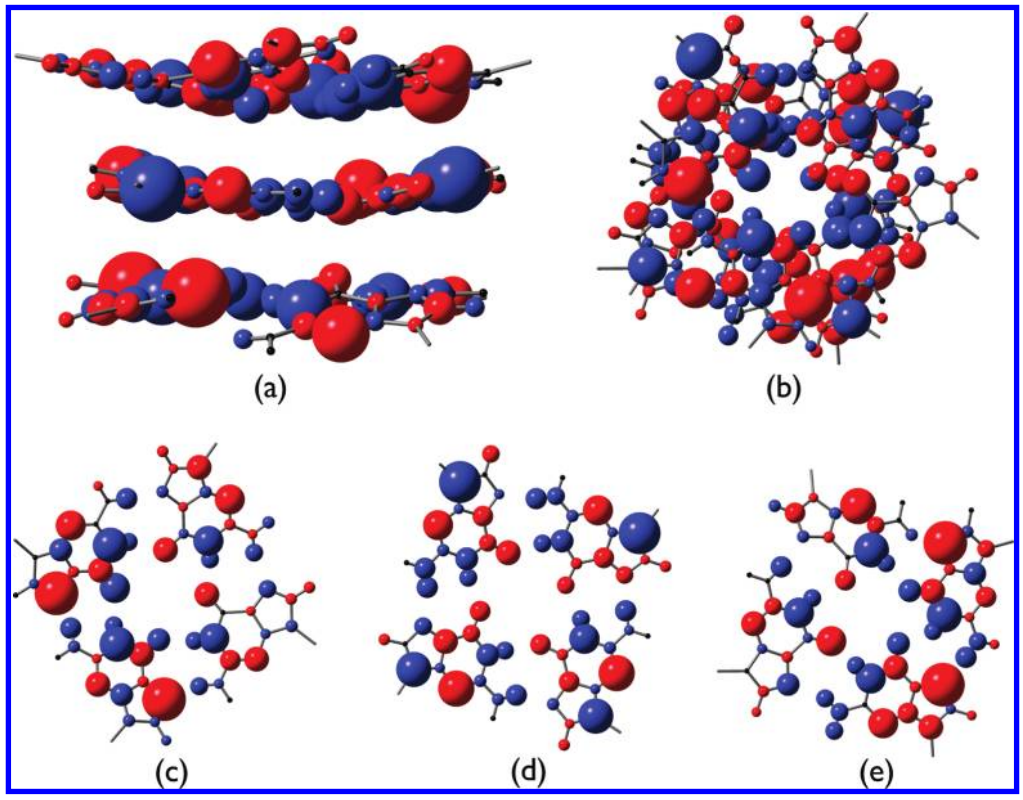

Figure 5. Graphical representation of the atomic energy differences, ΔE, for the stacked guanine quartets: (a) side view and (b) top view. The alternating pattern of stabilization and destabilization in the individual guanine quartets can be seen in the unstacked quartets: (c) top, (d) middle, and (e) bottom guanine quartets.

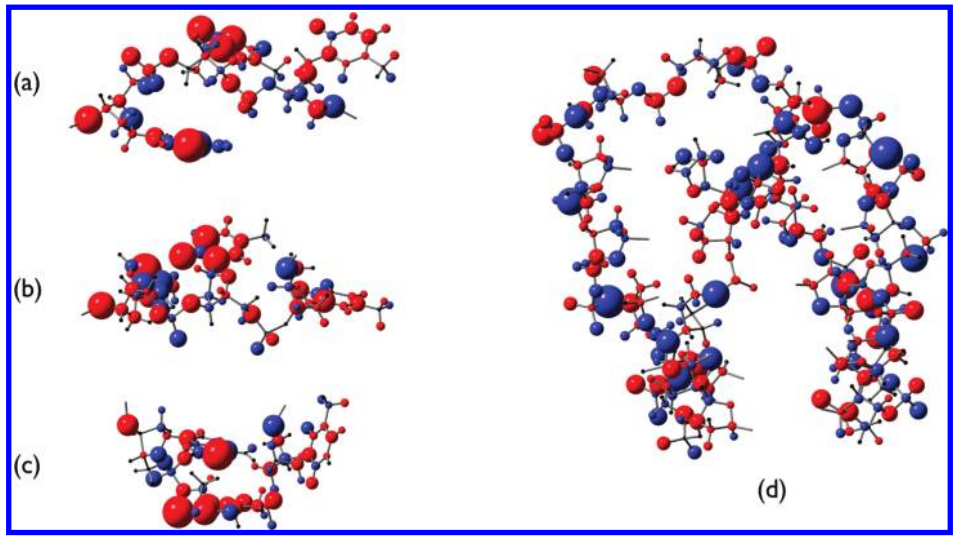

Figure 6. Graphical representation of the atomic energy differences, ΔE, for the loop segments and the sugar−phosphate backbone: (a) diagonal loop, T10T11A12, the lateral loops (b) T4T5A6 and (c) T16T17A18, and (d) the sugar−phosphate backbone.

guanine quartets exhibit an alternating pattern of stabilization and destabilization around the ring of the quartets. Furthermore, these regions actually overlap with one another when the quartets are stacked in the folded structure, giving the entire central guanine core an alternating pattern. In addition, the nucleobases in the TTA loop regions are largely stabilized upon folding, and the sugar−phosphate backbone throughout the whole structure exhibits relatively small changes in energy for the unfolded-to-folded transition. Overall, the folded guanine quadruplex is stabilized by −4523.3 kJ/mol relative to the unfolded, single-stranded telomere.

The inclusion of additional sodium cations within the quadruplex structure was also investigated. First, the results indicate that the sodium cations prefer to adopt a position between stacked guanine quartets or in the cavity formed by the external guanine quartets and the loop regions. Second, comparing the atomic energy differences of the systems with and without the sodium cations reveals that these ions have a large stabilizing effect for atoms located close to the cations, whereas the remainder of the quadruplex is relatively unaffected. Most notably, the carbonyl oxygen atoms of the guanine nucleobases exhibit the largest stabilization from these added cations, often upward of 100 kJ/mol per oxygen atom. Overall, the inclusion of the additional sodium cations imparts a further stabilization of upward of 2000 kJ/mol, depending on the number of cations included.

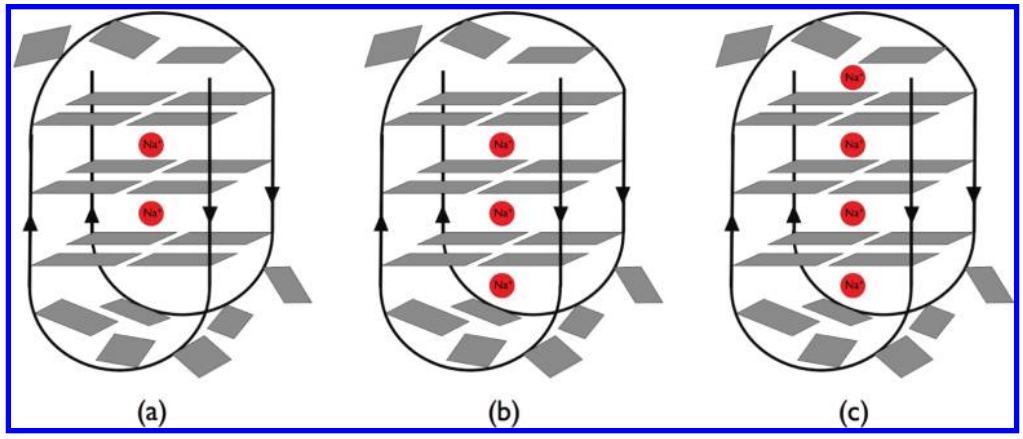

Figure 7. Schematic illustration of the location of the sodium cations (red spheres) in the structure containing (a) two Na^+ ions, (b) three Na^+ ions, and (c) four Na^+ ions.

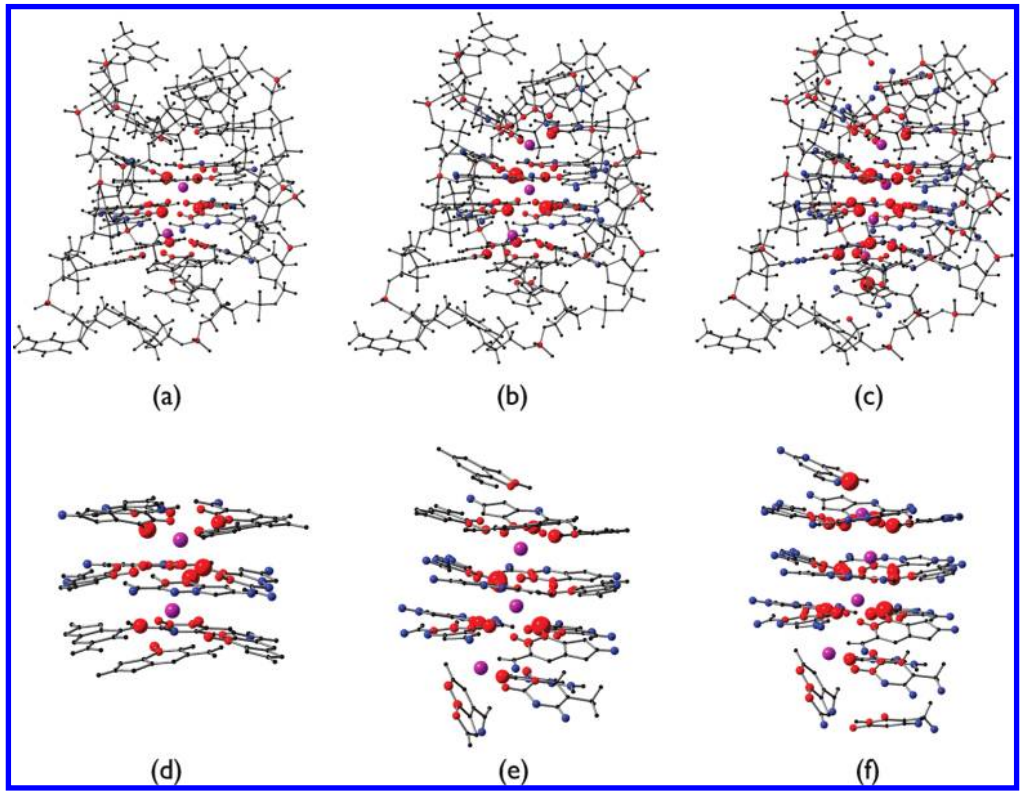

Figure 8. Graphical representation of the difference in atomic energy differences, $\Delta(\Delta E)$, for the quadruplex structures with additional sodium cations (purple spheres). Atoms that are stabilized in comparison to the quadruplex without sodium cations appear as red spheres; those that are destabilized appear as blue spheres; and those that are unaffected, as black spheres. The entire quadruplexes are shown for the systems with (a) two cations, (b) three cations, and (c) four cations. Images d, e, and f are enlargements of the nucleobases most largely affected for those same systems.

The results from this investigation have illustrated how each atom within the telomere is affected upon quadruplex formation. The three-dimensional representation of the atomic energy differences has allowed various trends to be elucidated. Ultimately, this detailed atomic information can help to guide future therapeutic endeavors, suggesting which regions of the quadruplex need to be stabilized to possibly enhance the formation of the quadruplex structures.

Acknowledgment. The authors acknowledge the Natural Sciences and Engineering Research Council of Canada (NSERC), Killam Trusts, the Walter C. Sumner Foundation, and Dalhousie University for financial support. We also thank ACEnet and WestGrid for additional computational resources. ACEnet is funded by the Canada Foundation for Innovation (CFI), the Atlantic Canada Opportunities Agency (ACOA), and the provinces of Newfoundland & Labrador, Nova Scotia, and New Brunswick. WestGrid is funded in part by the Canada Foundation for Innovation, Alberta Innovation and Science, BC Advanced Education, and the participating research institutions. WestGrid equipment is provided by IBM, Hewlett-Packard, and SGI. In addition, J.T. thanks the EU Marie Curie Transfer of Knowledge Programme for fellowship and project funding and acknowledges the Institute for Information Technology and Advanced Computation (IITAC), the Centre for Synthesis, and Chemical Biology (CSCB), the Higher Learning Authority (HEA) PRTLI scheme, the National Development Plan (NDP), and the Trinity Centre for High Performance Computing (TCHPC) for the provision of computational facilities.

Supporting Information Available: Schematic illustration of the numbering scheme used for the nucleobases and the quadruplex. Description of the fragmentation approach and a table indicating which nucleobases in the single-stranded telomere correspond to the nucleobases in the quadruplex. Atomic energy differences between the quadruplex and single-stranded telomere and the structural coordinates of the single-stranded DNA segment. This material is available free of charge via the Internet at http://pubs.acs.org.

References and Notes

(1) Blackburn, E. H. *Nature* **1991**, *350*, 569–573.
(2) Olovniko, A. M. *J. Theor. Biol.* **1973**, *41*, 181–190.
(3) Makarov, V. L.; Hirose, Y.; Langmore, J. P. *Cell* **1997**, *88*, 657–666.
(4) Wright, W. E.; Tesmer, V. M.; Huffman, K. E.; Levene, S. D.; Shay, J. W. *Genes Dev.* **1997**, *11*, 2801–2809.
(5) Gellert, M.; Lipsett, M. N.; Davies, D. R. *Proc. Natl. Acad. Sci. U.S.A.* **1962**, *48*, 2013–2018.
(6) Williamson, J. R.; Raghuraman, M. K.; Cech, T. R. *Cell* **1989**, *59*, 871–880.
(7) Davis, J. T. *Angew. Chem., Int. Ed.* **2004**, *43*, 668–698.
(8) Phan, A. T.; Kuryavyi, V.; Patel, D. J. *Curr. Opin. Struct. Biol.* **2006**, *16*, 288–298.
(9) Wen, J. D.; Gray, C. W.; Gray, D. M. *Biochemistry* **2001**, *40*, 9300–9310.
(10) Muniyappa, K.; Anuradha, S.; Byers, B. *Mol. Cell. Biol.* **2000**, *20*, 1361–1369.
(11) Mohaghegh, P.; Karow, J. K.; Brosh, R. M.; Bohr, V. A.; Hickson, I. D. *Nucleic Acids Res.* **2001**, *29*, 2843–2849.
(12) Sun, H.; Yabuki, A.; Maizels, N. *Proc. Natl. Acad. Sci. U.S.A.* **2001**, *98*, 12444–12449.
(13) Schaffitzel, C.; Berger, I.; Postberg, J.; Hanes, J.; Lipps, H. J.; Pluckthun, A. *Proc. Natl. Acad. Sci. U.S.A.* **2001**, *98*, 8572–8577.
(14) Paeschke, K.; Simonsson, T.; Postberg, J.; Rhodes, D.; Lipps, H. J. *Nat. Struct. Mol. Biol.* **2005**, *12*, 847–854.
(15) Cooke, H. J.; Smith, B. A. *Cold Spring Harbor Symp. Quant. Biol.* **1986**, *51*, 213–219.
(16) Harley, C. B.; Futcher, A. B.; Greider, C. W. *Nature* **1990**, *345*, 458–460.
(17) Hastie, N. D.; Dempster, M.; Dunlop, M. G.; Thompson, A. M.; Green, D. K.; Allshire, R. C. *Nature* **1990**, *346*, 866–868.
(18) Greider, C. W.; Blackburn, E. H. *Cell* **1985**, *43*, 405–413.
(19) Morin, G. B. *Cell* **1989**, *59*, 521–529.
(20) Shippenlentz, D.; Blackburn, E. H. *Science* **1990**, *247*, 546–552.
(21) Shay, J. W.; Bacchetti, S. *Eur. J. Cancer* **1997**, *33*, 787–791.
(22) Zahler, A. M.; Williamson, J. R.; Cech, T. R.; Prescott, D. M. *Nature* **1991**, *350*, 718–720.
(23) Read, M.; Harrison, R. J.; Romagnoli, B.; Tanious, F. A.; Gowan, S. H.; Reszka, A. P.; Wilson, W. D.; Kelland, L. R.; Neidle, S. *Proc. Natl. Acad. Sci. U.S.A.* **2001**, *98*, 4844–4849.
(24) Shin-ya, K.; Wierzba, K.; Matsuo, K.; Ohtani, T.; Yamada, Y.; Furihata, K.; Hayakawa, Y.; Seto, H. *J. Am. Chem. Soc.* **2001**, *123*, 1262–1263.
(25) Izbicka, E.; Wheelhouse, R. T.; Raymond, E.; Davidson, K. K.; Lawrence, R. A.; Sun, D. Y.; Windle, B. E.; Hurley, L. H.; Von Hoff, D. D. *Cancer Res.* **1999**, *59*, 639–644.
(26) Zaug, A. J.; Podell, E. R.; Cech, T. R. *Proc. Natl. Acad. Sci. U.S.A.* **2005**, *102*, 10864–10869.
(27) Oganesian, L.; Moon, I. K.; Bryan, T. M.; Jarstfer, M. B. *EMBO J.* **2006**, *25*, 1148–1159.
(28) Neidle, S.; Parkinson, G. *Nat. Rev. Drug Discovery* **2002**, *1*, 383–393.
(29) Hurley, L. H. *Nat. Rev. Cancer* **2002**, *2*, 188–200.
(30) Rezler, E. M.; Bearss, D. J.; Hurley, L. H. *Curr. Opin. Pharmacol.* **2002**, *2*, 415–423.
(31) Mergny, J. L.; Mailliet, P.; Lavelle, F.; Riou, J. F.; Laoui, A.; Helene, C. *Anti-Cancer Drug Des.* **1999**, *14*, 327–339.
(32) Binz, N.; Shalaby, T.; Rivera, P.; Shin-Ya, K.; Grotzer, M. A. *Eur. J. Cancer* **2005**, *41*, 2873–2881.
(33) Burger, A. M.; Dai, F. P.; Schultes, C. M.; Reszka, A. P.; Moore, M. J.; Double, J. A.; Neidle, S. *Cancer Res.* **2005**, *65*, 1489–1496.
(34) Pennarun, G.; Granotier, C.; Gauthier, L. R.; Gomez, D.; Boussin, F. D. *Oncogene* **2005**, *24*, 2917–2928.
(35) Moore, M. J. B.; Schultes, C. M.; Cuesta, J.; Cuenca, F.; Gunaratnam, M.; Tanious, F. A.; Wilson, W. D.; Neidle, S. *J. Med. Chem.* **2006**, *49*, 582–599.
(36) Zhou, J. M.; Zhu, X. F.; Lu, Y. J.; Deng, R.; Huang, Z. S.; Mei, Y. P.; Wang, Y.; Huang, W. L.; Liu, Z. C.; Gu, L. Q.; Zeng, Y. X. *Oncogene* **2006**, *25*, 503–511.
(37) Huppert, J. L.; Balasubramanian, S. *Nucleic Acids Res.* **2005**, *33*, 2908–2916.
(38) Todd, A. K.; Johnston, M.; Neidle, S. *Nucleic Acids Res.* **2005**, *33*, 2901–2907.
(39) Huppert, J. L.; Balasubramanian, S. *Nucleic Acids Res.* **2007**, *35*, 406–413.
(40) Eddy, J.; Maizels, N. *Nucleic Acids Res.* **2006**, *34*, 3887–3896.
(41) Wang, Y.; Patel, D. J. *Structure* **1993**, *1*, 263–282.
(42) Dewar, M. J. S.; Zoebisch, E. G.; Healy, E. F.; Stewart, J. J. P. *J. Am. Chem. Soc.* **1985**, *107*, 3902–3909.
(43) Dewar, M. J. S.; Zoebisch, E. G.; Healy, E. F.; Stewart, J. J. P. *J. Am. Chem. Soc.* **1993**, *115*, 5348–5348.
(44) Frisch, M. J.; Trucks, G. W.; Schlegel, H. B.; Scuseria, G. E.; Robb, M. A.; Cheeseman, J. R.; Montgomery, J. A., Jr.; Vreven, T.; Kudin, K. N.; Burant, J. C.; Millam, J. M.; Iyengar, S. S.; Tomasi, J.; Barone, V.; Mennucci, B.; Cossi, M.; Scalmani, G.; Rega, N.; Petersson, G. A.; Nakatsuji, H.; Hada, M.; Ehara, M.; Toyota, K.; Fukuda, R.; Hasegawa, J.; Ishida, M.; Nakajima, T.; Honda, Y.; Kitao, O.; Nakai, H.; Klene, M.; Li, X.; Knox, J. E.; Hratchian, H. P.; Cross, J. B.; Bakken, V.; Adamo, C.; Jaramillo, J.; Gomperts, R.; Stratmann, R. E.; Yazyev, O.; Austin, A. J.; Cammi, R.; Pomelli, C.; Ochterski, J. W.; Ayala, P. Y.; Morokuma, K.; Voth, G. A.; Salvador, P.; Dannenberg, J. J.; Zakrzewski, V. G.; Dapprich, S.; Daniels, A. D.; Strain, M. C.; Farkas, O.; Malick, D. K.; Rabuck, A. D.; Raghavachari, K.; Foresman, J. B.; Ortiz, J. V.; Cui, Q.; Baboul, A. G.; Clifford, S.; Cioslowski, J.; Stefanov, B. B.; Liu, G.; Liashenko, A.; Piskorz, P.; Komaromi, I.; Martin, R. L.; Fox, D. J.; Keith, T.; Al-Laham, M. A.; Peng, C. Y.; Nanayakkara, A.; Challacombe, M.; Gill, P. M. W.; Johnson, B.; Chen, W.; Wong, M. W.; Gonzalez, C.; Pople, J. A. *Gaussian 03, Revision B.05*; Gaussian, Inc.: Wallingford, CT, 2004.
(45) Hamprecht, F. A.; Cohen, A. J.; Tozer, D. J.; Handy, N. C. *J. Chem. Phys.* **1998**, *109*, 6264–6271.
(46) Johnson, E. R.; DiLabio, G. A. *Chem. Phys. Lett.* **2006**, *419*, 333–339.
(47) Biegler-Konig, F. W.; Bader, R. F. W.; Tang, T. *J. Comput. Chem.* **1982**, *3*, 317–328.
(48) Bader, R. F. W., *Atoms in Molecules: A Quantum Theory*; Oxford University Press: Oxford, U.K., 1990.
(49) Matta, C. F.; Boyd, R. J., *The Quantum Theory of Atoms in Molecules: From Solid State to DNA and Drug Design*; Wiley-VCH: Weinheim, 2007.
(50) Hanaoka, S.; Nagadoi, A.; Nishimura, Y. *Protein Sci.* **2005**, *14*, 119–130.
(51) Case, D. A.; Cheatham, T. E., III; Darden, T.; Gohlke, H.; Luo, R.; Merz, K. M.; Onufriev, A.; Simmerling, C.; Wang, B.; Woods, R. J. *J. Comput. Chem.* **2005**, *26*, 1668–1688.
(52) Case, D. A.; Darden, T. A.; Cheatham, T. E., III; Simmerling, C. L.; Wang, J.; Duke, R. E.; Luo, R.; Merz, K. M.; Pearlman, D. A.; Crowley, M.; Walker, R. C.; Zhang, W.; Wang, B.; Hayik, S.; Roitberg, A.; Seabra, G.; Wong, K. F.; Paesani, F.; Wu, X.; Brozell, S.; Tsui, V.; Gohlke, H.; Yang, L.; Tan, C.; Mongan, J.; Hornak, V.; Cui, G.; Beroza, P.; Mathews, D. H.; Schafmeister, C.; Ross, W. S.; Kollman, P. A. *AMBER 9*; University of California: San Francisco, 2006.
(53) Perez, A.; Marchan, I.; Svozil, D.; Sponer, J.; Cheatham, T. E.; Laughton, C. A.; Orozco, M. *Biophys. J.* **2007**, *92*, 3817–3829.
(54) Jorgensen, W. L.; Chandrasekhar, J.; Madura, J. D.; Impey, R. W.; Klein, M. L. *J. Chem. Phys.* **1983**, *79*, 926–935.
(55) Wang, J. M.; Cieplak, P.; Kollman, P. A. *J. Comput. Chem.* **2000**, *21*, 1049–1074.
(56) Shields, G. C.; Laughton, C. A.; Orozco, M. *J. Am. Chem. Soc.* **1998**, *120*, 5895–5904.
(57) Darden, T.; York, D.; Pedersen, L. *J. Chem. Phys.* **1993**, *98*, 10089–10092.
(58) Essmann, U.; Perera, L.; Berkowitz, M. L.; Darden, T.; Lee, H.; Pedersen, L. G. *J. Chem. Phys.* **1995**, *103*, 8577–8593.
(59) Feig, M.; Karanicolas, J.; Brooks, C. L. *J. Mol. Graph.* **2004**, *22*, 377–395.
(60) Meyer, M.; Suhnel, J. *J. Biomol. Struct. Dyn.* **2003**, *20*, 507–517.
(61) Meyer, M.; Suhnel, J. *J. Phys. Chem. A* **2003**, *107*, 1025–1031.
(62) van Mourik, T.; Dingley, A. J. *Chem.—Eur. J.* **2005**, *11*, 6064–6079.
(63) Davis, J. T.; Spada, G. P. *Chem. Soc. Rev.* **2007**, *36*, 296–313.
(64) Setnicka, V.; Novy, J.; Bohm, S.; Sreenivasachary, N.; Urbanova, M.; Volka, K. *Langmuir* **2008**, *24*, 7520–7527.
(65) Chowdhury, S.; Bansal, M. *J. Phys. Chem. B* **2001**, *105*, 7572–7578.
(66) Snoussi, K.; Halle, B. *Biochemistry* **2008**, *47*, 12219–12229.

JP912013K